THE JOURNAL OF BIOLOGICAL CHEMISTRY VOL. 281, NO. 15, pp. 9987–9995, April 14, 2006

Inhibition of S/G_2 Phase CDK4 Reduces Mitotic Fidelity*[S]

Received for publication, November 29, 2005, and in revised form, January 17, 2006 Published, JBC Papers in Press, February 13, 2006, DOI 10.1074/jbc.M512714200

Andrew Burgess[‡1], Matthew Wigan[‡], Nichole Giles[‡], Wanda DePinto[§], Paul Gillespie[¶], Frankie Stevens[‡], and Brian Gabrielli[‡2]

From the [‡]Cancer Biology Program, Centre for Immunology and Cancer Research, University of Queensland, Princess Alexandra Hospital, Brisbane, Queensland 4102, Australia and [§]Discovery Oncology and [¶]Discovery Chemistry, Hoffmann-La Roche Inc., Nutley, New Jersey 07110

Cyclin-dependent kinase 4 (CDK4)/cyclin D has a key role in regulating progression through late G_1 into S phase of the cell cycle. CDK4-cyclin D complexes then persist through the latter phases of the cell cycle, although little is known about their potential roles. We have developed small molecule inhibitors that are highly selective for CDK4 and have used these to define a role for CDK4-cyclin D in G_2 phase. The addition of the CDK4 inhibitor or small interfering RNA knockdown of cyclin D3, the cyclin D partner, delayed progression through G_2 phase and mitosis. The G_2 phase delay was independent of ATM/ATR and p38 MAPK but associated with elevated Wee1. The mitotic delay was because of failure of chromosomes to migrate to the metaphase plate. However, cells eventually exited mitosis, with a resultant increase in cells with multiple or micronuclei. Inhibiting CDK4 delayed the expression of the chromosomal passenger proteins survivin and borealin, although this was unlikely to account for the mitotic phenotype. These data provide evidence for a novel function for CDK4-cyclin D3 activity in S and G_2 phase that is critical for G_2/M progression and the fidelity of mitosis.

Cyclin-dependent kinase 4 (CDK4)[3] binds cyclin D to provide a mechanistic link between extracellular growth signals and the initiation of entry into S phase from G_0/G_1. Its role in this pathway is to phosphorylate and inactive members of the retinoblastoma protein (Rb) family, which includes Rb, p107, and p130 (1, 2). This phosphorylation allows the release and activation of E2F transcription factors, which in turn up-regulates the genes required for S phase. CDK4 is regulated by cyclin D binding, phosphorylation, and association with inhibitory protein subunits of the INK4 family. Unlike other CDK-cyclin complexes, it is present at constant levels throughout the cell cycle in continuously proliferating cells, although its activity varies.

Mutations in the CDK4-cyclin D/Rb pathway are commonly found in many types of cancer. A number of viral oncogenes directly target the inactivation of Rb, and overexpression of cyclin D is common in breast cancer. This is particularly relevant in melanoma, where germ line mutations of the cyclin-dependent kinase inhibitor $p16^{INK4A}$ or CDK4 mutations that disrupt p16 binding are carried in melanoma-prone kindred (for review, see Ref. 3). In addition, somatic $p16^{INK4A}$ loss or mutation occurs in up to 30% of melanomas (3, 4), and a small proportion of melanomas carry somatic CDK4 mutations that disrupt $p16^{INK4A}$ binding (4, 5). This points to the importance of the cyclin D/CDK4/Rb pathway in controlling G_0/G_1 cell cycle progression. However, the role of CDK4-cyclin D in the phosphorylation and inactivation of Rb can in some cases be effectively substituted by cyclin E-CDK2 (6), and knock-out mouse models have shown redundancy of CDK4 and CDK6, whereas knock-out of both had only minimal effect on the cell cycle of cells (7, 8). These data indicate that CDK4 is not essential for cell cycle progression, so then why is the CDK4-cyclin D pathway often de-regulated in cancer? An explanation may be that CDK4 has important functions in addition to the G_1 phase phosphorylation of Rb. A peak of CDK4-cyclin D3 activity has been demonstrated during S/G_2 phase (9), suggesting that there are likely to be additional functions and substrates for CDK4 outside of G_1 phase. This hypothesis is strengthened by the finding that CDK4-cyclin D3 can phosphorylate nucleolin, a protein that is implicated in the transcription and processing of ribosomal RNA and nucleolar structure as well as additional unidentified proteins (10).

To define the role for CDK4-cyclin D, we have produced small molecule inhibitors of CDK4-cyclin D and used siRNA knockdown of cyclin D3 to demonstrate specificity of the inhibitors. Using these, we demonstrate here that CDK4 plays a critical role in G_2/M phase progression. Loss of CDK4-cyclin D3 activity produced a transient delay in early G_2 phase before to the activation of CDK2-cyclin A in G_2 phase and CDK1-cyclin B1 at G_2/M. This delay does not appear to operate through the known G_2/M checkpoints mechanisms, the ATM/ATR, and the p38 MAPK mediated pathways that operate in response to a variety of cellular stresses. Inhibition of CDK4 also delayed transit through mitosis, with 30% of cells progressing through an aberrant mitosis to produce cells with multiple nuclei or containing micronuclei. We also observed a delay in the G_2/M phase expression of two gene products critical for the fidelity of partitioning of the replicated genome in mitosis, the chromosomal passenger proteins survivin and borealin. However, these proteins accumulated to relatively normal levels in cells that reached mitosis, suggesting that these were unlikely to contribute significantly to the aberrant mitosis observed. Our data indicate that inhibition of CDK4 activity during S and G_2 phase delays G_2/M progression and reduces the fidelity of mitosis, providing strong evidence that CDK4 plays an important role outside of G_1 and Rb phosphorylation.

EXPERIMENTAL PROCEDURES

Materials—Caffeine, the p38 MAPK inhibitor SB203580, and etoposide were purchased from Sigma-Aldrich. CDK4 inhibitors (RO 0506220 and RO 0505124) and two structurally similar compounds that show no CDK4 kinase inhibition (RO 0507574 and RO 0507304) were synthesized by Discovery Chemistry Group (Hoffmann-La Roche). All other chemicals used were of analytical grade.

* This work was supported in part by grants from the Queensland Cancer Fund and the National Health and Medical Research Council of Australia. The costs of publication of this article were defrayed in part by the payment of page charges. This article must therefore be hereby marked "*advertisement*" in accordance with 18 U.S.C. Section 1734 solely to indicate this fact.

[S] The on-line version of this article (available at http://www.jbc.org) contains supplemental Table 1.

[1] Current address: CNRS-CRBM, Montpellier 34293, France.

[2] An National Health and Medical Research Council Senior Research Fellow. To whom correspondence should be addressed. Fax: 61-7-3240-5946; E-mail: bgabrielli@cicr.uq.edu.au.

[3] The abbreviations used are: CDK4, cyclin-dependent kinase 4; CDK4i, CDK4 inhibitor; Rb, retinoblastoma protein; ATM, ataxia talengiectasia-mutated; ATR, ATM- and Rad3-related; GFP, green fluorescent protein; siRNA, small interfering RNA; BrdUrd, bromodeoxyuridine; FACS, fluorescence-activated cell sorter; FAM, 6 carboxyfluorescein; TAMRA, 6-carboxy-tetramethyl-rhodamine.

Cell Culture and Synchrony—All cells were cultured in Dulbecco's modified Eagle's medium (Invitrogen) supplemented with 3 mM HEPES and 10% (v/v) Serum Supreme (BioWhittaker) in tissue culture incubators set at 5% CO_2 and 37 °C. Hydroxyurea and double thymidine block release synchronizations were performed as described in Gabrielli *et al.* (11). Cells were treated with CDK4 inhibitors 1 h after release from synchrony unless stated otherwise and harvested at the indicated times. Growth assays were performed by 3-(4,5-dimethylthiazol-2-yl)-2,5-diphenyltetrazolium bromide (MTT) assay as described previously (12). Assays for mycoplasma were carried out monthly to ensure that all of the cultured cells were free of contamination.

CDK4 Inhibitor Kinase Screen—Kinase assays were performed by FlashPlate™ assays (PerkinElmer Life Sciences). FlashPlate assays were performed using recombinant human cyclin B-CDK1, human cyclin E-CDK2, or human cyclin D1-CDK4 complexes. Glutathione *S*-transferase (GST)-cyclin E, CDK2, GST-cyclin B, CDK1, GST-CDK4k, and cyclin D1 cDNA clones in baculovirus vectors were provided by Dr. W. Harper at the Baylor College of Medicine, Houston, TX. Proteins were co-expressed in High Five™ insect cells, and the complex was purified on glutathione-Sepharose resin (Amersham Biosciences). A 6×histidine-tagged truncated form of Rb protein (amino acid 386–928) was used as the substrate for the cyclin D1-CDK4, cyclin B-CDK1, and the cyclin E-CDK2 assays (the expression plasmid was kindly provided by Dr. Veronica Sullivan, Department of Molecular Virology, Roche Research Centre, Welwyn Garden City, UK). Protein expression was under the control of an isopropyl 1-thio-β-D-galactopyranoside-inducible promoter in an M15 *Escherichia coli* strain. Cells were lysed by sonication, and purification was carried out by binding lysates at pH 8.0 to a nickel-chelated agarose column pretreated with 1 mM imidazole. The resin was then washed several times with incrementally decreasing pH buffers to pH 6.0 and eluted with 500 mM imidazole. Eluted protein was dialyzed against 20 mM HEPES, pH 7.5, 30% glycerol, 200 mM NaCl, and 1 mM dithiothreitol. Purified Rb fusion protein stocks were quantitated for protein concentration, separated into aliquots, and stored at −70 °C.

For all three kinase assays, 96-well FlashPlates were coated with Rb protein at 10 μg/ml using 100 μl/well. Plates were incubated at 4 °C overnight or at room temperature for 3 h on a shaker. To control for nonspecific phosphorylation, one row of wells was coated with 100 μl/well coating buffer (20 mM HEPES, 0.2 M NaCl). Plates were then washed twice with wash buffer (0.01% Tween 20 in phosphate-buffered saline). Compounds to be tested were added to the wells at 5× final concentrations. Reactions were initiated by the immediate addition of 40 μl of reaction mix (25 mM HEPES, 20 mM $MgCl_2$, 0.002% Tween 20, 2 mM dithiothreitol, 1 μM ATP, 4 nM [^{33}P]ATP) and a sufficient amount of enzyme to give counts that are at least 10-fold above background. Plates were incubated at room temperature on a shaker for 30 min. Plates were washed four times with the wash buffer, sealed, and counted on the TopCount Scintillation Counter.

The protein kinase B, p38, and MAPK and tyrosine kinases were assayed in-house at Roche. Assays for these kinases are based on IMAP Technology™ (Molecular Device Corp.) that enables quantitation of kinase activity via preferential binding of phosphorylated fluorescent peptide substrates to immobilized metal beads. These reactions were carried out at ATP concentrations of 3× the K_m for the respective enzyme. Counter-screening against the other kinases was carried out using fluorescence resonance energy transfer assays at the K_m for ATP.

siRNA Design and Transfection—The Ambion Silencer siRNA construction kit (Ambion) was used to produce siRNAs against cyclin D3 and D1. The following target sequences were identified and appropriate oligonucleotides were constructed as per manufacturer's instructions. Three cyclin D3 target sequences were identified, and Blast searches were performed to ensure that the sequences did not contain significant homology to any other known genes. The sequences were: Sequence 1, AAGGATCTTTGTGGCCAAGGA; sequence 2, AAGATGCTGGCTTACTGGATG; sequence 3, AATTGGATACATACACCAGCA. All three produced similar levels of specific cyclin D3 knockdown, and siRNA against sequence 1 was then used for all remaining experiments. In addition, a scrambled version of sequence 1 (NS sequence, AAGAAGTTAGTCCGATGCGTG), which contained no homology to CDK4 or any known genes, was used as a control.

siRNA transfection were performed as per the manufacturer's instructions. Where indicated, cells were synchronized by blocking overnight with 2 mM hydroxyurea, and released into S phase the following day. They were then analyzed by live cell imaging, immunofluorescence, and immunoblotting.

RNA Isolation and cDNA Synthesis—Cells were lysed using TRIzol reagent (Invitrogen), and total RNA was extracted as per the manufacturer's instruction. The RNA was quantified by a Smart Spec spectrophotometer (Bio-Rad) at a wavelength of 260/280 nm, and the extract was stored at −70 °C until cDNA synthesis. cDNA was synthesized using Superscript III (Invitrogen) as per the manufacturer's instruction. An equal amount of total RNA was used for cDNA synthesis in each set of experiment.

Quantitative PCR—Quantitation of survivin cDNA and an internal reference cDNA (β-actin) was performed using a fluorescence based real-time detection method (ABI PRISM 7700 Sequence Detection System (Taqman), Applied Biosystems) as per the manufacturer's instruction. Briefly, a dual-labeled fluorescent oligonucleotide probe was used that annealed specifically within the forward and reverse primers. The PCR reaction consisted of 600 nM concentrations of each primer, 200 nM probe, 1× Taqman Universal PCR master mix containing 200 μM each dATP, dCTP, dGTP, 400 μM dUTP, 5.5 mM $MgCl_2$, 1 unit of AmpErase uracil *N*-glycosylase to a final volume of 20 μl (all reagents PerkinElmer Life Sciences). Cycling conditions were 50 °C for 2 min and 95 °C for 10 min followed by 40 cycles at 95 °C for 15 s and 60 °C for 1 min. The sequences for the PCR primers area as follows. Survivin: forward primer, 5′-TGCCCCGACGTTGCC-3′; reverse primer, 5′-CAGTTCTTGAATGTAGAGATGCGGT-3′; probe, 5′-(6-Fam)CCTGGCAGCCCTTTCTCAAGGACC-(Tamra)-3′. β-Actin: forward primer, 5′-AGCCTCGCTTTGCCGA-3′, reverse primer, 5′-CTGGTGCCTGGGGCG-3′, probe, 5′-(6-Fam)CCGCCGCCCGTCCACACCCGCC(Tamra)-3′.

Biochemical Analysis—Cells were lysed in NETN (20 mM Tris-HCl, pH 8, 1 mM EDTA, 100 mM NaCl, 0.5% Tween 20) supplemented with 150 mM NaCl, 10 mM NaF, 0.1 mM sodium orthovanadate, 1 mM phenylmethylsulfonyl fluoride, and protease inhibitor mixture (Sigma-Aldrich). After 20 min on ice, the DNA was pelleted, and lysates were resolved on appropriate SDS-polyacrylamide gel electrophoresis plates, transferred to nitrocellulose membranes, and immunoblotted for proteins using antibodies against borealin (a gift from Professor Earnshaw, Edinburgh (13)), pRb, Wee1, phosphotyrosine 15 CDK1/2 (PY15) (Cell Signaling), α-tubulin (Sigma-Aldrich), survivin, cyclin D3, cyclin A, CDK4, CDK2 (Santa Cruz Biotechnology), and cyclin B1 (11) using the appropriate horseradish peroxidase-conjugated secondary antibody (Zymed Laboratories Inc.) and enhanced chemiluminescence (PerkinElmer Life Sciences) for detection.

Immunofluorescent Staining—Cells were grown on glass coverslips. For immunostaining, cells were washed with phosphate-buffered saline, fixed with 100% −20 °C methanol, and stored at −20 °C until required. Coverslips were allowed to air-dry and then rehydrated with phosphate-buffered saline containing 0.1% Tween 20 and 3% bovine serum albumin

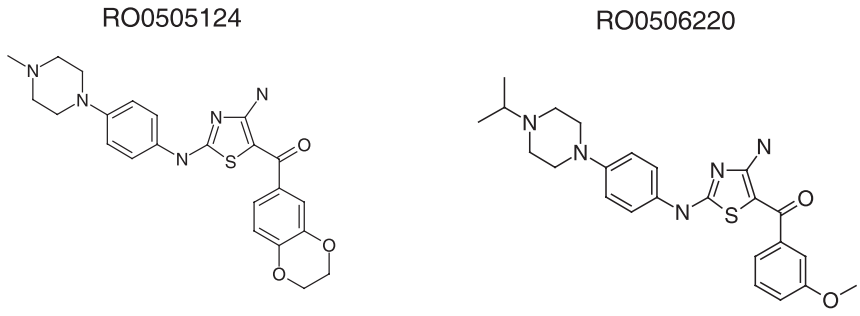

FIGURE 1. **The chemical structures for the two active CDK4 inhibitors RO0505124 and RO0506220 are shown.**

for 1 h at room temperature. The cells were stained with anti-α-tubulin, survivin, human autoimmune serum (h-ACA) to detect kinetochores, and 4,6-diamidino-2-phenylindole (0.1 μg/ml) for DNA. Coverslips were mounted on glass slides supplemented with Vectashield (Vector Laboratories, Burlingame, CA) to maintain fluorescence. Cells were visualized using a Carl Zeiss Axioskop 2 plus microscope, and images were captured using a Carl Zeiss AxioCam 2 camera and Axiovision and Adobe Photoshop software.

Flow Cytometry—For flow cytometric analysis (FACS), floating and attached cells were collected for analysis. Cells were fixed in ice-cold 70% ethanol and stored at −20 °C. Samples were then washed once in phosphate-buffered saline and re-suspended in DNA staining solution consisting of 5 μg/ml propidium iodide and RNase A (0.5 mg/ml) in phosphate-buffered saline. The stained cells were filtered through 37-μm silk gauze, and the single-cell suspensions were analyzed on a FACSCalibur (BD Biosciences) using Cell Quest, with the proportion of cells in each cell cycle stage and subdiploid population calculated using the ModFit analysis package (Verity Software House, Topsham, ME). Bromodeoxyuridine (BrdUrd) staining was performed as described previously (14) as was MPM-2 staining (15).

Live Cell Imaging—Cells were seeded the day before the experiment on 6- or 12-well plates at ~50% confluence. Live cell imaging was performed using a Zeiss Cell Observer. Images were captured every 10 min for the duration of the cell cycle using Zeiss Axiovision software. Single cell analysis was performed by individually following each cell through each frame and observing the number of frames required to complete each distinct phase. Entry into mitosis was identified when the cells rounded up, and exit from mitosis was when anaphase and cytokinesis were observed.

RESULTS

Identification of Highly Selective Small Molecule Inhibitors of CDK4—The diaminothiazole series of compounds were identified as a result of a screen for cyclin-cyclin-dependent kinase inhibitors (see "Experimental Procedures" for details of the screen). Modifications to the compound class produced two potent and selective CDK4 inhibitors with IC_{50} values of 20 nM for recombinant CDK4-cyclin D *in vitro* that were >100-fold more potent for CDK4 compared with CDK1 and 2 *in vitro* (Fig. 1, Table 1). The inhibitors are reversible and bind the ATP pocket of the kinases. A screen of 128 protein kinases was performed commercially using RO0505124 at a 1 μM concentration to assess the potential number of kinases that may be inhibited by these compounds. Eleven kinases from different families were inhibited >90% at this dose, demonstrating the relatively high degree of selectivity of the drugs but indicating that other kinases may also be targets. To demonstrate that these compounds inhibit CDK4 in cells, a number of cell lines with or without functional Rb were tested. Inhibition of CDK4 should produce a G_1 delay and reduction in Rb phosphorylation in cells that contain functional Rb. HeLa cells that do not contain functional Rb did not display a G_1 arrest after 24 h of treatment with 2 μM RO0506220, whereas

TABLE 1
***In vitro* inhibition of kinases by CDK4i**

Kinase	Inhibition IC_{50}	
	RO0505124	RO0506220
	nM	
CDK4-cyclin D	20	20
CDK2-cyclin E	2,360	4,144
CDK1-cyclin B	3,042	1,973
c-Met	>20,000	>20,000
Src	3,210	3,480
Lck	>100,000	>100,000
Insulin-like growth factor 1 receptor	22,000	20,000
Insulin receptor	71,000	24,000
p38 MAPK	29,000	>100,000
Protein kinase B/AKT	>200,000	>200,000
c-Jun NH_2-terminal kinase	>50,000	>50,000
Extracellular signal-regulated kinase 1	>100,000	>100,000

SK-Mel-13 cells that have functional Rb had a strong G_1 arrest (Fig. 2*A*). Similar data were obtained with both RO0506220 and RO0505124, whereas the inactive analogues had no effect on either cell lines. Later experiments were performed with RO0506220 and RO0505124 and are denoted as CDK4 inhibitor (CDK4i). Asynchronously growing HCT-116 cells, which contain functional Rb, were treated for 24 h with increasing doses of CDK4i. Cells were then either pulsed with BrdUrd and harvested for FACS analysis, or samples were collected to examine Rb phosphorylation status. A dose of 3.9 μM was required to reduce S phase to 50% of control levels (IC_{50}), with a significant reduction in the level of Rb phosphorylation also observed (Fig. 2, *B* and *C*). Higher doses further inhibited BrdUrd incorporation and Rb phosphorylation. These data demonstrated that drug treatment arrested cells in G_1 phase, blocking progression into S phase. Interestingly, the proportion of G_2/M phase cells appeared to either remain constant or increased after CDK4i treatment, whereas it would be expected to decrease if the drugs caused only a G_1 phase arrest. An additional 9 cell lines were tested, and the IC_{50} values for inhibition of S phase in these cells ranged from 0.5 to 8 μM (Table 2). The much higher drug concentrations required for the *in vivo* inhibition of CDK4 activity compared with *in vitro* is likely to be a consequence of nonspecific binding of the drugs reducing their effective concentrations. At IC_{50} concentrations the drugs caused little toxicity even after 3 days of treatment. Higher doses caused a moderate increased toxicity. To avoid any potentially nonspecific toxic effects, a dose of 2–4 μM CDK4i was chosen as an appropriate concentration for the remainder of the experiments, as this provided strong *in vivo* inhibition of CDK4 without affecting CDK1 or CDK2 activity.

Inhibition of CDK4 Delays Cells in G_2 Phase—Previous work had provided evidence that CDK4-cyclin D3 was active in S and G_2 phases and that inhibiting this activity caused a G_2/M phase delay (9). To analyze the effects of the CDK4 inhibitors on cell cycle progression beyond the Rb-dependent G_1 arrest, cells were synchronized and then treated during early S phase with CDK4i. The progression of cells through the remainder of the cell cycle was monitored using flow cytometry, biochemical analysis, and time-lapse microscopy. Upon release, cells were

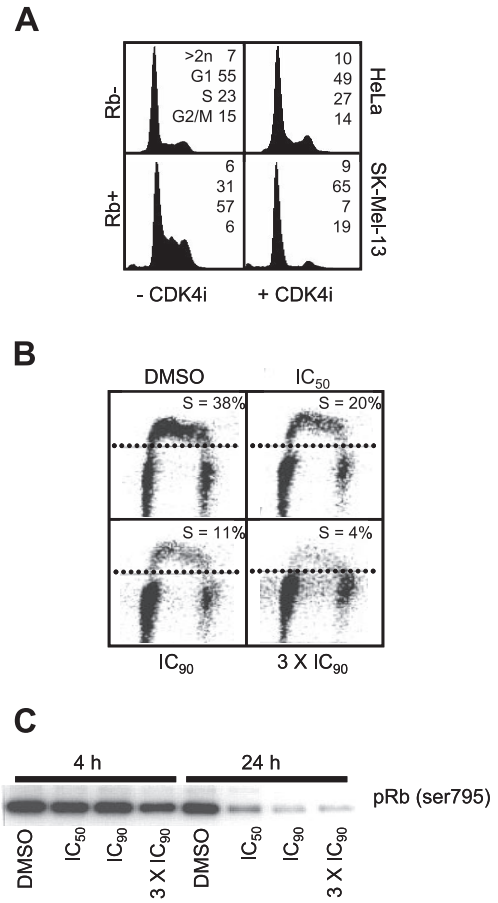

FIGURE 2. **CDK4 Inhibitors Causes a G_1 arrest in an Rb-dependent manner.** *A*, asynchronously growing HeLa cells (Rb-deficient) and melanoma cell line SK-Mel-13 (Rb-competent) were treated for 24 h with 2 μM CDK4i or inactive analogue (*−CDK4i*) then analyzed by FACS for DNA content. The percentage in each cell cycle phase and sub-diploid (<2 *n*), representing the dead population, is shown. *B*, asynchronous cultures of HCT-116 cells were treated with increasing doses of CDK4i for 24 h. Cells were then incubated with BrdUrd for 30min before harvesting for FACS. The percentage of cells staining positive for BrdUrd is indicated. IC_{50} for RO05050124 used in this experiment was 3.9 μM; IC_{90} was 6.1 μM. *DMSO*, dimethyl sulfoxide. *C*, asynchronous HCT-116 cells were treated with increasing doses of CDK4i as in panel *B* for either 4 or 24 h before harvesting for immunoblot analysis with phospho-Rb (Ser-795).

TABLE 2

CDK4i inhibits proliferation of cell lines

Proliferation was measured by 3-(4,5-dimethylthiazol-2-yl)-2,5-diphenyltetrazolium bromide (MMT) assay 48 h after drug addition. The data are the mean of two separate determinations performed in duplicate.

Cell line	Inhibition IC_{50}	
	RO0505124	RO0506220
	μM	
Colon		
HCT116	3.85	1.10
RKO	1.60	0.54
SW480	3.67	1.06
COLO205	2.04	0.56
Breast		
MDA-MB-435	3.06	1.20
MDA-MB-453	1.45	0.71
Lung		
H460a	8.12	1.14

treated at various stages through S phase with or without 2 μM CDK4i or inactive control. Treatment 2 h post-release during early S phase resulted in HeLa cells delaying progression through mitosis by 4 h. These cells remained in G_2/M at 12 h post-release when the untreated controls had progressed through mitosis to the subsequent G_1 phase (Fig. 3*A*). A dose of 4 μM increased the G_2/M delay to >4 h. The ability of CDK4i to inhibit G_2/M progression was also observed with two other cell lines, the melanoma cell lines A2058 and SK-Mel-13 (Fig. 3*B*). The latter has a functional Rb-dependent G_1 arrest, whereas the former is defective for the checkpoint. There was little effect on S phase progression observed with any of the cell lines examined. The G_2/M delay was dependent on the addition of CDK4i during early S phase. The addition during mid-S phase (4 h) produced a shorter delay of up to 2 h, whereas the addition in late S/G_2 phase (6 h) had no effect on progression through G_2/M (Fig. 3*A*, data for A2058 and SKMel-13 not shown). Treatment with inactive analogues had no effect on cell cycle progression.

To determine whether the G_2/M delay was during G_2 phase or mitosis, MPM-2 FACS was performed to specifically define the mitotic population. Control HeLa cells had begun to enter into mitosis by 8 h and returned to G_1 by 12 h, whereas cells treated with CDK4i delayed entry into mitosis until 12 h post-release. This indicated that CDK4i-treated cells were delayed in G_2 phase (Fig. 3*C*). This G_2 delay was confirmed by cyclin A-CDK2 and cyclin B1-CDK1 kinase assays. The delay corresponded to an accumulation of phosphotyrosine 15 CDK1 and CDK2 observed by immunoblotting with a phosphospecific antibody (Fig. 3*D*). Cyclin B1 accumulated normally in the CDK4i-treated cultures (Fig. 3*D*) as did cyclin A (see Fig. 7*A*); thus, the blockade was due to failure to dephosphorylate the inhibitory phosphotyrosine 15 residue on CDK2 and CDK1. The activation of the G_2 phase pool of cyclin A-CDK2 and G_2/M cyclin B1-CDK1 in CDK4i-treated cultures was also delayed compared with untreated controls (data not shown). The inhibition of phosphotyrosine 15 dephosphorylation on both CDK1 and CDK2 was similar to that observed in the G_2 arrests imposed by DNA damaging agents such as ionizing radiation, etoposide, and ultraviolet radiation (16), which utilize stress checkpoint signaling pathways involving either ATM, ATR, or p38 MAPK (17, 18). The addition of either caffeine to inhibit ATM/ATR signaling or the p38 MAPK inhibitor SB203580 had no effect on the G_2 delay observed with CDK4i addition. However, both these drugs did advance entry into mitosis in the controls by 1 h (Fig. 3*E*). The lack of effect of either inhibitor on the CDK4i-induced G_2 delay suggests that does not operate through known DNA damage or stress checkpoint pathways. When the level of the Wee1 kinase, which phosphorylates the inhibitory tyrosine 15 residue on CDK1 and CDK2, was examined, it was found to decrease in inactive compound-treated controls as they progressed into mitosis as expected, but in CDK4i-treated samples Wee1 levels appeared to increase and stabilize for the duration of the G_2 phase delay, which may represent an alternative mechanism by which the G_2 delay was imposed (Fig. 3*F*).

The fate of individual cells after CDK4i treatment as they progressed into and through mitosis was examined using time-lapse microscopy. Control cells entered mitosis at 8–9 h post-release with a high degree of synchrony. In contrast, CDK4i-treated cells began entry into mitosis 11 h post-release (Fig. 4*A*). There was also a difference in the time the cells remained in mitosis, with control cells requiring 78 ± 51 min to reach anaphase/telophase, whereas CDK4i-treated cells required 152 ± 97 min. The broader spread of time required to reach anaphase was due to a subpopulation of cells that delayed longer in mitosis (Fig. 4*B*). In addition, 20% of cells failed to undergo cytokinesis correctly in the CDK4i-treated cultures, with the cells re-joining and forming large multinuclear cells (Fig. 4*C*). This was only rarely observed in the control cultures.

Specific siRNA Knockdown of Cyclin D3 Produces a Similar G_2 Delay—Although a panel of more than 80 protein kinases were examined for inhibition by the two CDK4i, it is still possible that the delay seen was due to an unknown effect of the drug. To exclude this possibility, siRNA knockdown

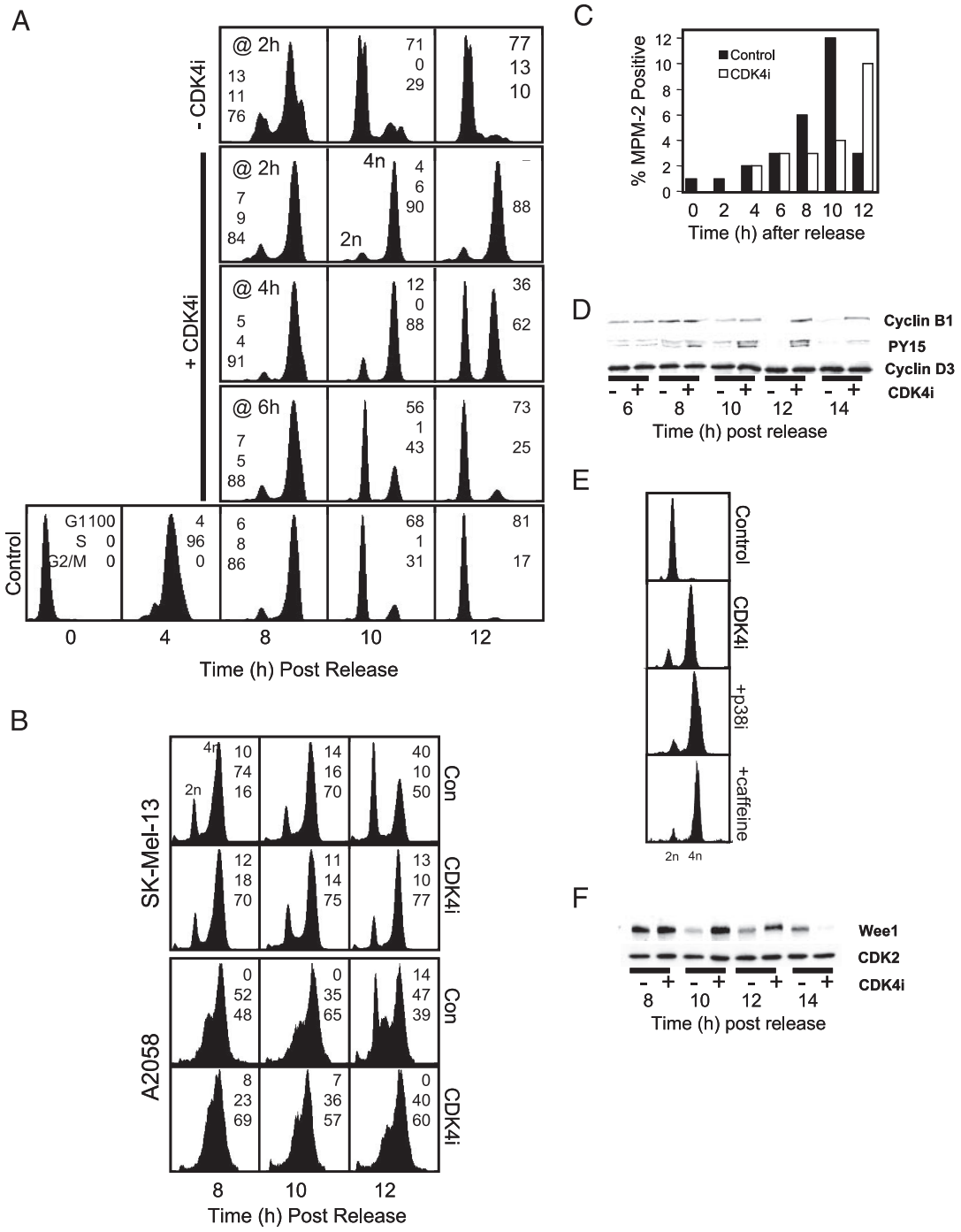

FIGURE 3. **Inhibition of CDK4 results in a G_2 delay.** *A*, HeLa cells were synchronized using a double thymidine block release method. Cells were treated at 2, 4, and 6 h post-release with 2 μM CDK4i with 2 μM inactive analogue (−*CDK4i*) or without (*Control*). A slow down through G_2/M phase is observed when the drug was added before 4 h post-release. *B*, A2058 and SK-Mel-13 cells were synchronized using 2 mM hydroxyurea. 1 h after release cells were treated with 2 μM CDK4i or without (*Con*) and then harvested for DNA FACS at the indicated times post-release. The proportion of G_1, S phase, and G_2/M phase cells is indicated. *C*, HeLa cells were synchronized using a double thymidine block release method. At 1 h post-release they were treated with 2 μM CDK4i. Cells were then harvested at the indicated times post-release and analyzed for MPM-2 positive cells and DNA content using FACS. *D*, synchronized HeLa cells treated with CDK4i in early S phase or untreated controls were harvested at the indicated times after release and analyzed by immunoblotting for cyclin B1, phosphotyrosine 15 CDK1/2 (*PY15*), or cyclin D3 as a loading control. Peak mitosis was at 9–10 h in the controls and 12–14 h in CDK4i treated cultures. *E*, synchronized HeLa cells treated with either inactive compound or CDK4i in early S phase and 20 μM p38 MAPK inhibitor SB203580 (*p38i*) or 5 mM caffeine to inhibit ATM/ATR activity was added at 8 h after synchrony release (G_2 phase), then harvested at 12 h after release for FACS analysis. In this experiment peak mitosis was at 10 h. *F*, similar samples to those used in *D* were immunoblotted for Wee1.

of cyclin D3, the partner of G_2 phase CDK4 identified in previous studies (9), was used to inhibit CDK4 activity, and the effects on G_2/M progression was assessed. Three siRNA were designed against target sequences in the C-terminal, N-terminal, central region of cyclin D3. All three siRNAs produced specific knockdown of cyclin D3 at a concentration of 10–20 nM at 24 h post-transfection, with protein levels beginning to recover by 48 h (Fig. 5, *A* and *B*). The levels of cyclin D1, E, A (not shown), and B1 (Fig. 5*A*) remained unaffected by the siRNA transfection, indicating that the knockdown was specific for cyclin D3. The three cyclin D3 siRNA produced similar cell cycle effects so only the data for siRNA number 1 is shown. To examine the effect of cyclin D3 knockdown in synchronized, transfected HeLa cells, FACS analysis and time-lapse microscopy was performed. The

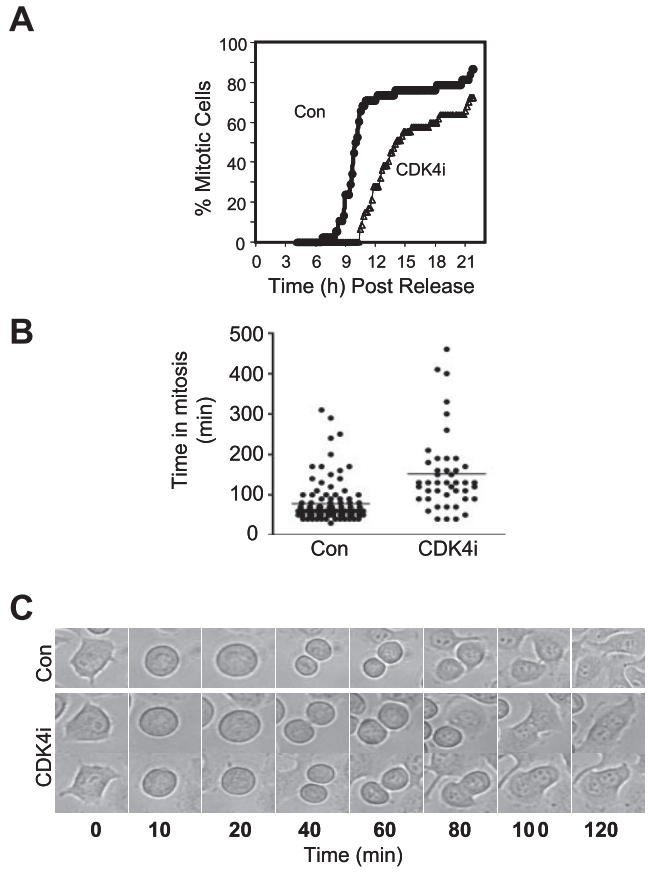

FIGURE 4. **Inhibition of CDK4 affects G_2/M progression.** *A*, time-lapse microscopy was performed on synchronized HeLa cells treated with or without 2 μM CDK4i. Mitotic entry counts were then performed with ~50 cells per field, scored with a minimum of 3 independent fields for both control (*Con*) and CDK4i-treated cells counted. This is representative of three separate experiments. *B*, time required for cells to progress through mitosis until anaphase is shown. These data are representative of three separate experiments. *C*, time lapse sequence of either control or CDK4i-treated cells progressing into and through mitosis. The two CDK4i-treated cells progressed through mitosis with similar timing to the control, but these cells both failed cytokinesis and eventually rejoined to form a single binuclear cell.

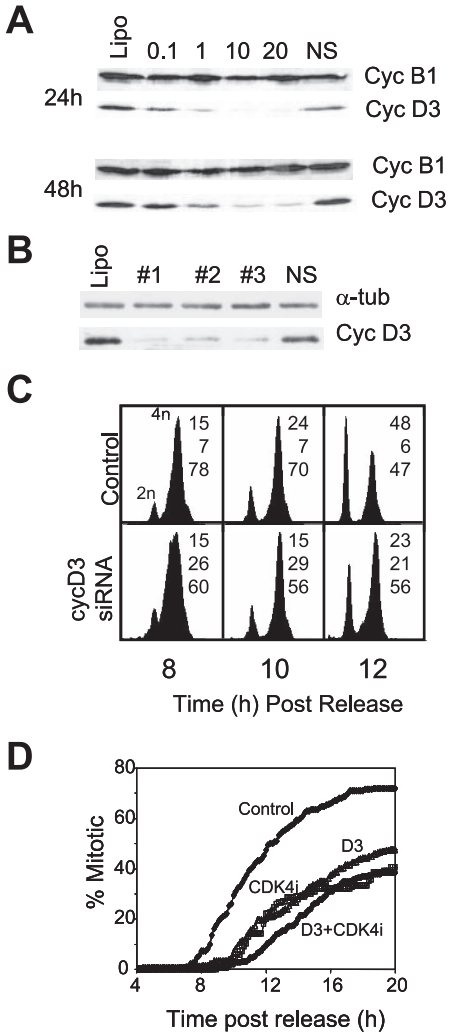

FIGURE 5. **siRNA knockdown of cyclin D3 phenocopies CDK4i.** *A*, HeLa cells were transfected with various doses of cyclin D3 siRNA number 1, 20 nM concentrations of a nonsense scrambled version of the cyclin D3 siRNA (*NS*) or without any siRNA (*Lipo*) and harvested 24 and 48 h post-transfection. Cell lysates were immunoblotted for cyclin D3 and cyclin B1, which served as both a loading and siRNA specificity control. *B*, HeLa cells were transfected with 20 nM concentrations of each of the three different cyclin D3 siRNAs, then harvested at 24 h and immunoblotted for cyclin D3 knockdown. *C*, HeLa cells transfected with 20 nM cyclin D3 siRNA number 1 or with a scrambled siRNA (*Control*), then synchronized using hydroxyurea. After release, cells were harvested at the indicated time points for FACS analysis of DNA content. *D*, synchronized HeLa cells were either untreated (*Control*) or treated with CDK4i, cyclin D3 siRNA number 1 (D3), or CDK4i and siRNA, and their progression into mitosis was followed by time lapse microscopy.

results were essentially identical to the CDK4i-treated cells. Cyclin D3 knockdown delayed entry into mitosis by more than 2 h compared with control cells (Fig. 5, *C* and *D*). To demonstrate that the delay observed with the CDK4i was due to specific inhibition of CDK4, synchronized cultures treated with both CDK4i and cyclin D3 siRNA were analyzed by time-lapse microscopy. Simultaneous treatment with CDK4i and cyclin D3 knockdown produced an only slightly longer delay than the individual treatments, probably due to less than complete inhibition of CDK4 with the individual treatments (Fig. 5*C*). The lack of additive effect of the CDK4i and cyclin D3 knockdown demonstrated that the CDK4i drugs specifically inhibited CDK4-cyclin D3 activity that was responsible for the cell cycle delays observed.

CDK4-inhibited Cells Undergo Aberrant Mitosis—Time-lapse data revealed that 20% of CDK4i-treated cells failed to undergo mitosis correctly, forming large multinuclear cells, suggesting that drug treatment disrupted normal mitosis. Control and drug- and siRNA-treated cultures were fixed as they progressed through mitosis, stained for microtubules and DNA, and examined by fluorescence microscopy. Both control and CDK4i-treated cells had well-formed bipolar mitotic spindles. However, 40% of CDK4i-treated cells displayed an aberrant mitotic phenotype, characterized by lagging chromosomes, which often decorated the astral side of the spindle microtubules (Fig. 6, *A* and *B*). These lagging chromosomes were also visualized by time-lapse microscopy of GFP-H2B-expressing HeLa cells, where these chromosomes formed micronuclei after mitotic exit (Fig. 6*C*). A similar spectrum and level of mitotic aberrations was observed in the cyclin D3 siRNA-treated cells (data not shown). Examination of cells at 24 h after synchrony release when the majority of cells have returned to interphase revealed that 30% of CDK4i-treated cells contained multiple nuclei and micronuclei compared with 10% in control cultures (Fig. 6*D*). These nuclear defects are an indicator of mitotic failure and were likely to be the consequence of the failed mitosis.

Inhibition of S/G_2 CDK4/Cyclin D3 Delays Expression of Chromosomal Passenger Proteins—The failure of mitosis and defects in cytokinesis detected by time lapse and fluorescent microscopy suggested that there were possibly defects in the mechanisms controlling the fidelity of mitosis, either the spindle assembly checkpoint or the chromosomal passenger proteins such as survivin, aurora B, or borealin, which form a complex with INCENP at the centromere that

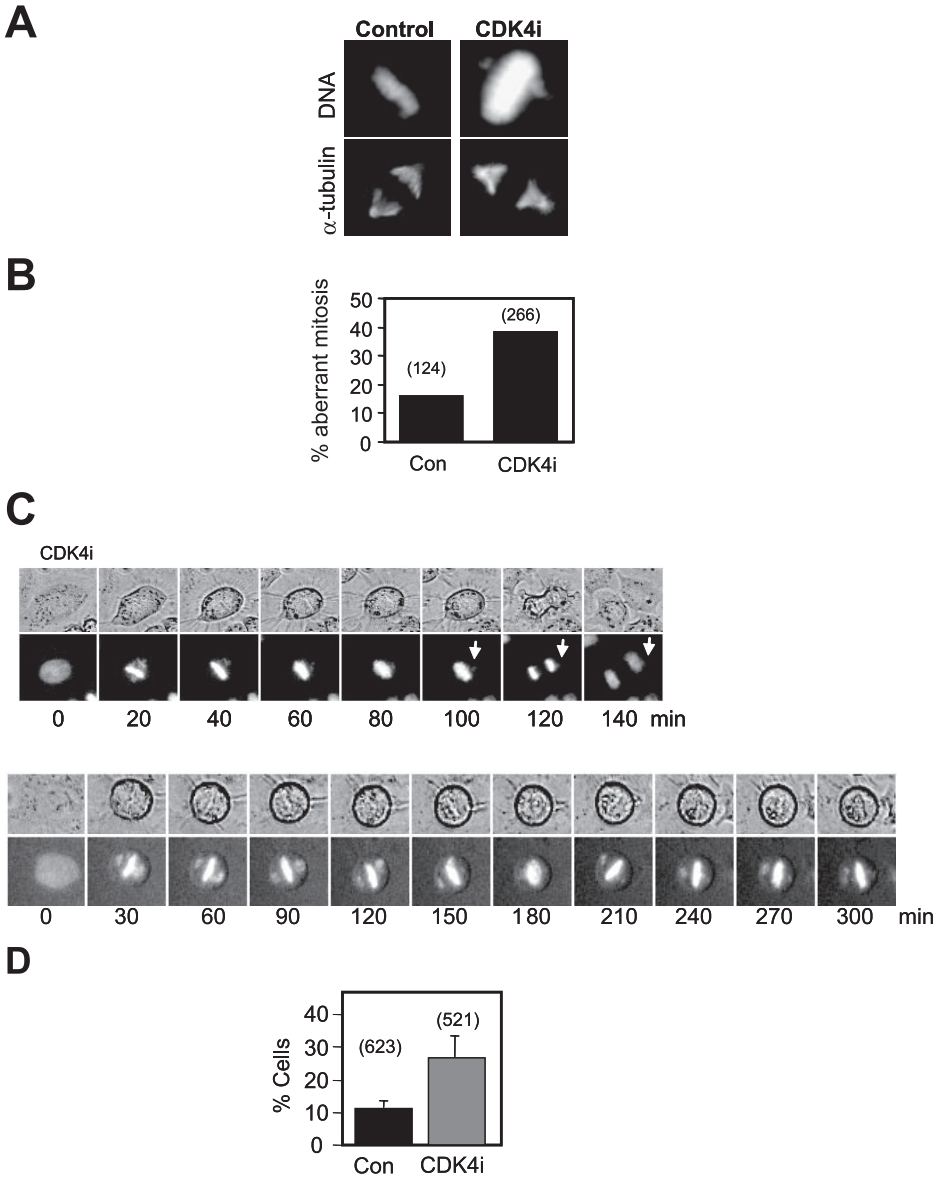

FIGURE 6. **CDK4i induce an aberrant mitosis.** *A*, HeLa cells were grown on coverslips and synchronized using a double thymidine block release. At 1 h post-release they were treated with 2 μM of CDK4i. Coverslips were harvested, and cells were fixed as they progressed into mitosis, ~9 and 12 h post-release for control and CDK4i-treated cells, respectively. Cells were then stained for α-tubulin and 4,6-diamidino-2-phenylindole for DNA. *B*, cell counts were performed on mitotic cells from *A*. Each cell was visually inspected for normal metaphase congression or the presence of lagging chromosomes, and the percentage of aberrant mitosis is reported. The number of mitotic cells counted is shown in *parentheses*. *C*, two CDK4i-treated GFP-H2B-expressing HeLa cells progressing through mitosis. Note that the cells delayed in mitosis for an extended period compared with controls. In the *top panel* a chromosome fragment fails to congress to the metaphase plate and forms a micronucleus in one of the daughter cells (indicated with the *white arrow*). In the *bottom panel* chromosome fragments that fail to congress are clearly seen. *D*, cells were treated as describe in *A* but were harvested 24 h after release. Interphase cells were then examined for the presence of multi- and micro nuclei and chromosome bridges, as indicators of progression though an aberrant mitosis. These data represent the three individual experiments and are presented as the percentage of total cells examined. The total number of cells counted is shown in *parentheses*.

influences spindle checkpoint function (19). The mitotic delay detected after CDK4i treatment indicated that the spindle checkpoint was functioning, and CDK4i treatment did not affect the ability of nocodazole to arrest cells in mitosis (data not shown). However, the presence of cells with multiple nuclei and micronuclei is evidence that cells exited mitosis prematurely, indicating that the checkpoint eventually failed. Knockdown of survivin or borealin or inhibition of aurora B activity result in similar mitotic aberrations and failure of cytokinesis as seen with CDK4i (13, 20, 21). Examination of total levels of survivin revealed that the normal G_2/M accumulation of survivin protein, which peaked at 10 h, was delayed in the drug-treated cells (Fig. 7*A*). In controls, survivin continued to accumulate until peak mitosis 10 h in this experiment, when cyclin A levels started to diminish. In CDK4i-treated cells, survivin levels did not reach control mitotic levels even at 14 h, which corresponded to peak mitosis. When the levels of three of the mitotic passenger proteins were examined in a separate experiment, the accumulation of both survivin and borealin were delayed and failed to reach control mitotic levels (Fig. 7*B*). The level of aurora B was unchanged across mitosis, and CDK4i treatment had no affect. Similar results were obtained using cyclin D3 knockdown (Fig. 7*C*). To determine whether the delay and reduction in survivin accumulation in CDK4-inhibited cells was due to reduced transcription, real time RT-PCR analysis of the mRNA levels of survivin was performed. In control cells the expected increase in survivin mRNA was observed, with the peak corresponding to peak mitosis at 12 h (Fig. 7*D*). In both the CDK4i- and siRNA-treated cells there was little reduction in survivin mRNA levels, although these remained elevated longer probably due to the delay in mitosis. Borealin mRNA behaved in an identical manner (data not shown).

The localization of survivin is very characteristic, accumulating at the centromeres in early mitosis then relocating to the midline of the cells on the mid-spindle during anaphase and telophase, then decorating the midbody in cytokinesis (19, 22). All of the chromosomal passenger proteins localize identically through mitosis (19). Immunofluorescent staining of mitotic cells for survivin did reveal an increased proportion of mitotic cells with low levels of survivin staining and aberrant mitosis (Fig. 8*A*). When the cells with low survivin levels were quantitated, the proportion displaying aberrant mitosis increased from 9% in controls to 18% in CDK4i-treated cultures, but

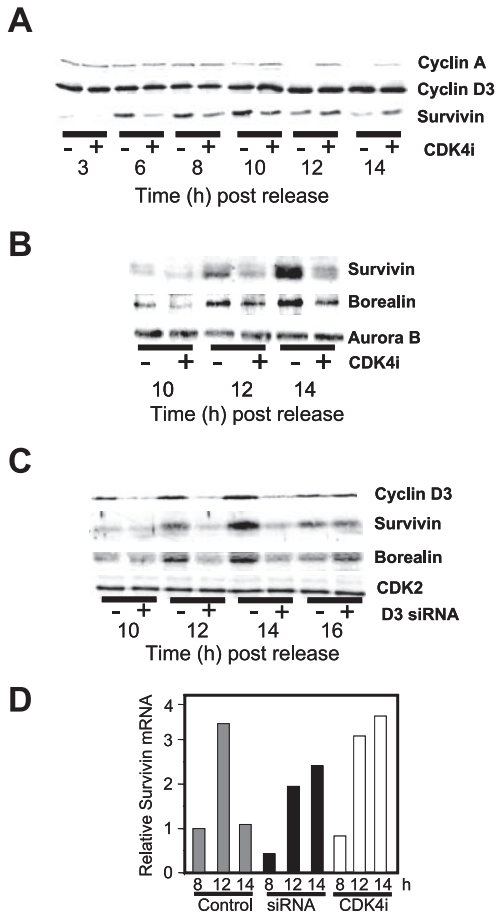

FIGURE 7. **CDK4i treatment delayed and reduced the accumulation of survivin and borealin.** *A*, HeLa cells were synchronized using a double thymidine block release and treated with 2 μM CDK4i in early S phase. Cells were harvested at the indicated times post-release for immunoblot analysis of the indicated proteins. Cyclin D 3 was used as a loading control. This is representative of five separate experiments. *B*, in an experiment similar to *A*, lysates were immunoblotted for the levels of the indicated chromosomal passenger proteins. In this experiment peak mitosis was at 10–12 h in the controls and 13–14 h in the CDK4i-treated cultures. *C*, synchronized HeLa cells either pretreated with cyclin D3 siRNA number 1 or scramble siRNA were harvested at the indicated times after synchrony release and immunoblotted for the indicated proteins. CDK2 was used as a loading control. Peak mitosis was at 12 h in the scrambled control and 14 h in the cyclin D3 siRNA treated cultures. *D*, quantitative real time RT-PCR for survivin was performed using mRNA prepared from samples from the experiment shown in *B*. The data are the average of triplicate determination. These data are representative of three separate experiments.

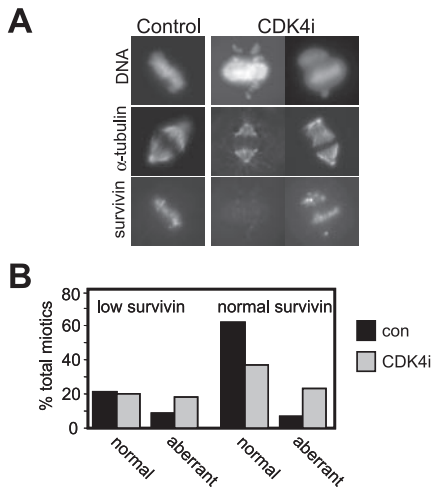

FIGURE 8. **CDK4i does not affect mitotic levels of survivin.** *A*, immunofluorescence of either control or CDK4i-treated cells stained for DNA, microtubules (α-tubulin), and survivin. These represent typical normal survivin staining (control and *right column* of CDK4i-treated) and low survivin staining (*left column* of CDK4i-treated). *B*, percentage of cells displaying normal or aberrant mitotic phenotype and their level of survivin staining. 124 controls (*con*) and 266 CDK4i-treated mitotic cells were counted.

there was a similarly increased proportion of cells with normal survivin staining and aberrant mitosis, from 7% in controls to 23% with CDK4i treatment (Fig. 8*B*). This suggests that reduced chromosomal passenger protein levels are unlikely to be the major determinant of the aberrant mitosis in CDK4i-treated cells.

DISCUSSION

The function of CDK4-cyclin D has been defined in terms of its G_1 phase role in regulating the activity of pocket proteins and thereby controlling the transcription of genes required for progression into S phase. However, there is evidence of a role for CDK4 later in the cell cycle. CDK4 activity has been demonstrated in S and G_2 phase (9, 23, 24), and this activity is inhibited in UV-irradiated G_2 phase-delayed cells, associated with increased $p16^{INK4A}$ and loss of CDK4 phosphorylation (9). We have now demonstrated that inhibition of CDK4-cyclin D activity using either highly selective low molecular weight inhibitors or by siRNA knockdown of the S/G_2 phase CDK4 cyclin partner, cyclin D3, causes a delay in entry into mitosis. The specificity of the drugs for inhibiting CDK4-cyclin D3 in S/G_2 phase was demonstrated by the similarity of the effects of CDK4i addition and siRNA knockdown of cyclin D3, the CDK4 partner in S/G_2 phase. Furthermore, we have used three different cyclin D3 target sequences to knock down cyclin D3, which all produced similar cell cycle effects. Finally, CDK4i addition to cyclin D3 knockdown cells did not significantly increase the G_2 delay observed with either treatment alone, indicating they both inhibit the same target.

The G_2 phase delay corresponds to a block in the cdc25-dependent activation of CDK2-cyclin A and CDK1-cyclin B, similar to the genotoxin-induced G_2 delay reported previously (16). Surprisingly, it does not appear to be imposed by the characterized G_2 checkpoint mechanisms involving ATM/ATR or p38 MAPK. Interestingly, an increase in the level of the CDK inhibitory kinase Wee1 was detected. This simply may be a consequence of inhibition of proteasome-mediated destruction, which normally occurs as cells enter mitosis (25). However, a similar accumulation of Wee1 has been reported elsewhere, and it may represent an alternative target for G_2 checkpoint controls (26). The length of the delay is dependent on the degree of CDK4 inhibition, as doubling the dose of CDK4i significantly increased the duration of G_2 delay up to 12 h in some experiments, suggesting that CDK4 activity is rate limiting for G_2/M progression. Thus, inhibition of CDK4-cyclin D3 activity during S and G_2 phase does delay G_2-phase progression. However, the mechanism of the delay is at present unclear. This suggests that CDK4-cyclin D3 has an important function during S phase that directly impacts on G_2/M progression.

The effect of inhibition of CDK4-cyclin D3 activity on mitosis was unexpected. Inhibition resulted in a significant increase in the proportion of cells undergoing an aberrant mitosis characterized by lagging chromosomes. This generally was only one or two chromosomes as compared with the major failure of chromosome congression at metaphase observed with either mutation, inhibition of kinetochore-associated mitotic spindle checkpoint-associated proteins (21, 27, 28), or drugs that affect chromatin structure (14). The lagging chromosomes initiate a mitotic checkpoint delay, demonstrated by the increased time the CDK4i-treated cells require to reach anaphase. Immunostaining for the presence of MAD2, a spindle checkpoint component, revealed its localization to the kinetochores of lagging chromosomes, a marker of activation of the spindle assem-

bly checkpoint (29).[4] However, the spindle checkpoint eventually fails as there was a significant increase in the proportion of cells that exited mitosis without properly segregating their chromosomes, evident as cells with multiple and micronuclei. This appears to be an example of mitotic slippage where the spindle checkpoint is initiated but fails to maintain the arrest, resulting in cells prematurely exiting mitosis (30) (31). The chromosomal passenger complex consisting of INCENP, aurora B, survivin, and borealin, influences the localization and operation of the kinetochore-associated mitotic spindle checkpoint components such as MAD2 and BUBR1, thereby affecting spindle checkpoint function (13, 19–21). The chromosomal passengers accumulate at the centromere in prophase of mitosis, and each chromosomal passenger influences the localization and activity of the other passenger proteins (19). We have found that G_2/M phase accumulation of two of the chromosomal passenger complex, survivin and borealin, was delayed, but there was little reduction in the levels of survivin or borealin that localized at centromeres of mitotic cells after CDK4i treatment, indicating that these proteins are likely to function normally. The reduced accumulation of these proteins observed by immunoblotting is likely the consequence of a loss of synchrony of the CDK4i-treated samples. The level of aurora B was unaffected after CDK4i treatment, and we found no effect on aurora B activity with normal levels of histone H3 Ser10 phosphorylation detected (data not shown). Thus, the mechanism by which S/G_2 CDK4-cyclin D3 influences the fidelity of mitosis remains unclear. However, it does appears not to involve regulating the expression of the chromosomal passenger protein.

A possible explanation for the mitotic defects is that they are a consequence of a failure to stably arrest in G_2 phase after CDK4i treatment. Mitotic defects are a common feature of cells that fail to stably arrest after exposure to ultraviolet radiation (32) or treatment with histone deacetylase inhibitors (14). In these cases it is likely that some form of either DNA damage or defective chromatin structure is responsible for the mitotic defects. The source of defects after CDK4i treatment is at present unclear.

The regulation of the CDK4-cyclin D/p16^{INK4A} axis is often disrupted in a wide variety of cancers, particularly melanomas, by either mutation deletion or overexpression of various components (4). This has generally been attributed to dysregulation of the G_1-phase Rb-dependent checkpoint. Although there is no doubt of the importance of this effect, it is also possible that dysregulation of CDK4 may influence other cell cycle phases. In this report we have demonstrated that CDK4 has a critical role in ensuring the fidelity of mitotic partitioning of the replicated genome. We have previously reported that in epidermal-derived cell lines that the S/G_2 phase CDK4 activity is inhibited by increased p16^{INK4A} levels in response to suberythemal doses of ultraviolet radiation (9) and that increased p16^{INK4A} expression correlated with a G_2 phase delay in irradiated human skin (33, 34). Inhibition of CDK4-cyclin D3 activity can delay progression through G_2 and is likely to contribute to the G_2 delay observed after exposure to ultraviolet radiation. P16^{INK4A} inhibition of CDK4 in this response may also regulate pathways that influence the fidelity of mitosis. The failure to inhibit CDK4-cyclin D3 may result in cells that are capable of transiting mitosis with mutant DNA and surviving to pass their mutations to future generations, thereby contributing to melanoma.

[4] M. Wigan, F. Stevens, and B. Gabrielli, unpublished observations.

Acknowledgments—We thank Robyn Warrener for the gift of the GFP-H2B-expressing HeLa cells and Associate Professor Elizabeth Musgrove and Dr. Graeme Walker for critical reading of the manuscript. We thank Prof. W. C. Earnshaw for the borealin antibody.

REFERENCES

1. Kato, J. Y., and Sherr, C. J. (1993) *Proc. Natl. Acad. Sci. U. S. A.* **90,** 11513–11517
2. Ezhevsky, S. A., Nagahara, H., Vocero-Akbani, A. M., Gius, D. R., Wei, M. C., and Dowdy, S. F. (1997) *Proc. Natl. Acad. Sci. U. S. A.* **94,** 10699–10704
3. Hayward, N. K. (2003) *Oncogene* **22,** 3053–3062
4. Castellano, M., Pollock, P. M., Walters, M. K., Sparrow, L. E., Down, L. M., Gabrielli, B. G., Parsons, P. G., and Hayward, N. K. (1997) *Cancer Res.* **57,** 4868–4875
5. Wolfel, T., Hauer, M., Schneider, J., Serrano, M., Wolfel, C., Klehmann-Hieb, E., De Plaen, E., Hankeln, T., Meyer zum Buschenfelde, K. H., and Beach, D. (1995) *Science* **269,** 1281–1284
6. Keenan, S. M., Lents, N. H., and Baldassare, J. J. (2004) *J. Biol. Chem.* **279,** 5387–5396
7. Kozar, K., and Sicinski, P. (2005) *Cell Cycle* **4,** 388–391
8. Malumbres, M., Sotillo, R., Santamaria, D., Galan, J., Cerezo, A., Ortega, S., Dubus, P., and Barbacid, M. (2004) *Cell* **118,** 493–504
9. Gabrielli, B. G., Sarcevic, B., Sinnamon, J., Walker, G., Castellano, M., Wang, X. Q., and Ellem, K. A. (1999) *J. Biol. Chem.* **274,** 13961–13969
10. Prall, O. W. J., Sarcevic, B., Musgrove, E. A., Watts, C. K. W., and Sutherland, R. L. (1997) *J. Biol. Chem.* **272,** 10882–10894
11. Gabrielli, B. G., De Souza, C. P., Tonks, I. D., Clark, J. M., Hayward, N. K., and Ellem, K. A. (1996) *J. Cell Sci.* **109,** 1081–1093
12. Burgess, A. J., Pavey, S., Warrener, R., Hunter, L. J., Piva, T. J., Musgrove, E. A., Saunders, N., Parsons, P. G., and Gabrielli, B. G. (2001) *Mol. Pharmacol.* **60,** 828–837
13. Gassmann, R., Carvalho, A., Henzing, A. J., Ruchaud, S., Hudson, D. F., Honda, R., Nigg, E. A., Gerloff, D. L., and Earnshaw, W. C. (2004) *J. Cell Biol.* **166,** 179–191
14. Qiu, L., Burgess, A., Fairlie, D. P., Leonard, H., Parsons, P. G., and Gabrielli, B. G. (2000) *Mol. Biol. Cell* **11,** 2069–2083
15. Krauer, K. G., Burgess, A., Buck, M., Flanagan, J., Sculley, T. B., and Gabrielli, B. (2004) *Oncogene* **23,** 1342–1353
16. Goldstone, S., Pavey, S., Forrest, A., Sinnamon, J., and Gabrielli, B. (2001) *Oncogene* **20,** 921–932
17. O'Connell, M. J., Walworth, N. C., and Carr, A. M. (2000) *Trends Cell Biol.* **10,** 296–303
18. Bulavin, D. V., Amundson, S. A., and Fornace, A. J. (2002) *Curr. Opin. Genet. Dev.* **12,** 92–97
19. Vagnarelli, P., and Earnshaw, W. C. (2004) *Chromosoma* (*Berl.*) **113,** 211–222
20. Carvalho, A., Carmena, M., Sambade, C., Earnshaw, W. C., and Wheatley, S. P. (2003) *J. Cell Sci.* **116,** 2987–2998
21. Ditchfield, C., Johnson, V. L., Tighe, A., Ellston, R., Haworth, C., Johnson, T., Mortlock, A., Keen, N., and Taylor, S. S. (2003) *J. Cell Biol.* **161,** 267–280
22. Li, F., Ackermann, E. J., Bennett, C. F., Rothermel, A. L., Plescia, J., Tognin, S., Villa, A., Marchisio, P. C., and Altieri, D. C. (1999) *Nat. Cell Biol.* **1,** 461–466
23. Bates, S., Parry, D., Bonetta, L., Vousden, K., Dickson, C., and Peters, G. (1994) *Oncogene* **9,** 1633–1640
24. Matsushime, H., Quelle, D. E., Shurtleff, S. A., Shibuya, M., Sherr, C. J., and Kato, J. Y. (1994) *Mol. Cell. Biol.* **14,** 2066–2076
25. Watanabe, N., Arai, H., Iwasaki, J., Shiina, M., Ogata, K., Hunter, T., and Osada, H. (2005) *Proc. Natl. Acad. Sci. U. S. A.* **102,** 11663–11668
26. Papi, M., Berdougo, E., Randall, C. L., Ganguly, S., and Jallepalli, P. V. (2005) *Nat. Cell Biol.* **7,** 1029–1035
27. Chan, G. K., Jablonski, S. A., Sudakin, V., Hittle, J. C., and Yen, T. J. (1999) *J. Cell Biol.* **146,** 941–954
28. Taylor, S. S., and McKeon, F. (1997) *Cell* **89,** 727–735
29. Waters, J. C., Chen, R. H., Murray, A. W., and Salmon, E. D. (1998) *J. Cell Biol.* **141,** 1181–1191
30. Rieder, C. L., and Maiato, H. (2004) *Dev. Cell* **7,** 637–651
31. Weaver, B. A., and Cleveland, D. W. (2005) *Cancer Cell* **8,** 7–12
32. Milligan, A., Gabrielli, B. G., Clark, J. M., N. K., H., and Ellem, K. A. O. (1998) *Mutat. Res.* **422,** 43–53
33. Pavey, S., Conroy, S., Russell, T., and Gabrielli, B. (1999) *Cancer Res.* **59,** 4185–4189
34. Pavey, S., Russell, T., and Gabrielli, B. (2001) *Oncogene* **20,** 6103–6110
35. Fabian, M. A., Biggs, W. H., III, Treiber, D. K., Atteridge, C. E., Azimioara, M. D., Benedetti, M. G., Carter, T. A., Ciceri, P., Edeen, P. T., Floyd, M., Ford, J. M., Galvin, M., Gerlach, J. L., Grotzfeld, R. M., Herrgard, S., Insko, D. E., Insko, M. A., Lai, A. G., Lelias, J. M., Mehta, S. A., Milanov, Z. V., Velasco, A. M., Wodicka, L. M., Patel, H. K., Zarrinkar, P. P., and Lockhart, D. J. (2005) *Nat. Biotechnol.* **23,** 329–336

Supplementary Table 1

The Cdk4 inhibitor, RO0505124, was screened against Ambit's panel of 128 kinases (35). A primary screen was performed at 1 micromolar, and the results reported as '% Competition'. High scores indicate strong screening hits. For kinases not hit in the primary screen at this concentration, a score of '<50' was assigned. Quantitative binding constants (K_d's) were not determined on any of the kinases scored as hits in the primary screen.

Kinase Target Ambit Gene Symbol	% Competition @ 1 μM
AAK1	84
ABL1	<50
ABL2	<50
ACK1	<50
AKT1	<50
AMPK-alpha1	<50
AURKA	<50
AURKC	<50
BIKE	<50
BLK	<50
BMX	<50
BRAF	<50
BRAF(V600E)	<50
BTK	<50
CAMK1	<50
CAMK1D	<50
CAMK1G	<50
CAMK2A	<50
CAMK2B	<50
CAMK2D	<50
CAMK2G	<50
CAMKK1	<50
CAMKK2	<50
CDK5	<50
CLK1	100
CLK2	100
CLK3	89
CLK4	97
CSK	<50
CSNK1E	<50
CSNK1G1	98
CSNK1G2	99
CSNK2A1	<50
DAPK2	<50
DAPK3	<50
DMPK	<50
EGFR	<50
EPHA2	<50
EPHA3	<50
EPHA4	<50
EPHA5	<50
EPHA6	<50
EPHA7	<50

EPHA8	<50
EPHB1	<50
EPHB4	<50
ERBB2	<50
ERBB4	<50
ERK2	<50
FER	<50
FES	<50
FGFR1	<50
FGFR2	<50
FGFR3	<50
FGR	<50
FLT3	<50
FLT4	<50
FRK	<50
FYN	<50
GAK	100
HCK	<50
IGF1R	<50
INSR	<50
ITK	<50
JAK1(Kin.Dom.1)	94
JAK2(Kin.Dom.2)	<50
JNK1	<50
JNK2	<50
JNK3	66
KIT	<50
LCK	<50
LIMK1	<50
LTK	<50
LYN	<50
MAP3K4	<50
MAP4K5	<50
MARK2	<50
MKNK2	<50
MYLK2	<50
NEK2	<50
NEK6	<50
NEK9	<50
p38-alpha	<50
p38-beta	<50
p38-gamma	<50
PAK1	<50
PAK3	<50
PAK4	<50
PAK6	<50
PAK7/PAK5	<50
PCTK1	99
PDGFRA	<50
PDGFRB	<50
PDPK1	<50
PHKG1	<50
PHKG2	<50
PIM2	<50

PKAC-alpha	<50
PKMYT1	<50
PLK4	<50
PTK2	<50
PTK2B	<50
PTK6	<50
RAF1	<50
RIPK2	<50
ROS1	<50
RPS6KA2(Kin.Dom.1)	<50
RPS6KA3(Kin.Dom.1)	<50
RPS6KA5(Kin.Dom.1)	<50
SLK	99
SRC	<50
STK10	<50
STK11	<50
STK16	87
STK17A	89
STK17B	<50
STK3	<50
STK36	86
STK4	<50
SYK	<50
TIE2	<50
TNIK	<50
TRKA	<50
TTK	78
TXK	<50
ULK3(mouse)	<50
VEGFR2	<50
YES	<50

Inhibition of S/G_2 Phase CDK4 Reduces Mitotic Fidelity

Andrew Burgess, Matthew Wigan, Nichole Giles, Wanda DePinto, Paul Gillespie, Frankie Stevens and Brian Gabrielli

J. Biol. Chem. 2006, 281:9987-9995.
doi: 10.1074/jbc.M512714200 originally published online February 13, 2006
